Erschienen in: Optical Materials Express ; 4 (2014), 7. - S. 1336-1344

Optical properties of $LiInSe_2$ in the THz frequency regime

Qijun Liang,[1] Shanpeng Wang,[2,*] Xutang Tao,[2] and Thomas Dekorsy[1,3]

[1]*Department of Physics and Center for Applied Photonics, University of Konstanz, D-78457 Konstanz, Germany*
[2]*State Key Lab of Crystal Materials, Shandong University, 250100 Jinan, China*

[3]*thomas.dekorsy@uni-konstanz.de*

[*]*wshp@sdu.edu.cn*

Abstract: We investigate the optical properties of $LiInSe_2$ (LISe) by THz time-domain spectroscopy (THz-TDS). The experimental results indicate that LISe has excellent transparency in the THz frequency region. We determine quantitatively the birefringence of LISe. The refractive index and absorption coefficient along the three dielectric axes of LISe are reported in the THz frequency region. The lattice vibrations of LISe are analyzed on the basis of the THz-TDS measurement in combination with infrared and Raman spectra. The origin of the low-frequency vibrational modes below 3 THz as interatomic bond-bending modes is revealed.

OCIS codes: (300.6495) Spectroscopy, terahertz; (160.4760) Optical properties; (160.4330) Nonlinear optical materials; (260.1440) Birefringence.

References and links

1. J. Lloyd-Hughes and T.-I. Jeon, "A review of the terahertz conductivity of bulk and nano-materials," J. Infrared. Milli. Terahz Waves **33**(9), 871–925 (2012).
2. R. Ulbricht, E. Hendry, J. Shan, T. F. Heinz, and M. Bonn, "Carrier dynamics in semiconductors studied with time-resolved terahertz spectroscopy," Rev. Mod. Phys. **83**(2), 543–586 (2011).
3. K. Wiesauer and C. Jördens, "Recent advances in birefringences studies at THz frequencies," J. Infrared. Milli. Terahz Waves **34**(11), 663–681 (2013).
4. E. Tupitsyn, P. Bhattacharya, E. Rowe, L. Matei, M. Groza, B. Wiggins, A. Burger, and A. Stowe, "Single crystal of $LiInSe_2$ semiconductor for neutron detector," Appl. Phys. Lett. **101**(20), 202101 (2012).
5. F. W. Ohrendorf and H. Haeuseler, "Lattice dynamics of chalcopyrite type compounds part IV. Calculations of TO phonon modes in a reduced rigid ion model," Cryst. Res. Technol. **35**(5), 569–578 (2000).
6. Y. Li, W. Fan, H. Sun, X. Cheng, P. Li, and X. Zhao, "First-principles study of the electronic, optical, and lattice dynamics properties of $LiInSe_2$ polymorph," J. Appl. Phys. **106**(3), 033704 (2009).
7. T. Ma, C. Yang, Y. Xie, L. Sun, W. Lv, R. Wang, C. Zhu, M. Wang, "Electronic and optical properties of orthorhombic $LiInS_2$ and $LiInSe_2$: A density functional theory investigation," Comput. Mater. Sci. **47**, 99 (2009).
8. O. Balachninaite, L. Petraviciute, M. Maciulevicius, V. Sirutkaitis, L. Isaenko, S. Lobanov, A. Yelisseyev, J.-J. Zondy, "Optical characterization of the $LiInS_2$ and $LiInSe_2$ crystals," Proc. of SPIE **6596**, 65961J (2007).
9. T. Kamijoh, T. Nozaki, and K. Kuriyama, "Dielectric constants and bond parameters of $LiInSe_2$ and $LiGaSe_2$," J. Appl. Phys. **53**(1), 761–763 (1982).
10. S. Wang, X. X. Zhang, X. Zhang, C. Li, Z. Gao, Q. Lu, X. Tao, "Modified Bridgman growth and properties of mid-infrared $LiInSe_2$ crystal," DOI: 10.1016/j.jcrysgro.2014.02.043, J. Cryst. Growth (2014).
11. L. Isaenko, A. Yelisseyev, S. Lobanov, V. Petrov, F. Rotermund, G. Slekys, and J.-J. Zondy, "$LiInSe_2$: A biaxial ternary chalcogenide crystal for nonlinear optical applications in the midinfrared," J. Appl. Phys. **91**(12), 9475–9480 (2002).
12. P. Y. Yu and M. Cardona, *Fundamentals of Semiconductors: Physics and Materials Properties* (Springer, 2001).

#208591 - $15.00 USD Received 20 Mar 2014; revised 5 May 2014; accepted 6 May 2014; published 6 Jun 2014

13. R. Gebs, G. Klatt, C. Janke, T. Dekorsy, and A. Bartels, "High-speed asynchronous optical sampling with sub-50fs time resolution," Opt. Express **18**(6), 5974–5983 (2010).
14. A. Dreyhaupt, S. Winnerl, T. Dekorsy, and M. Helm, "High-intensity terahertz radiation from a microstructured large-area photoconductor," Appl. Phys. Lett. **86**(12), 121114 (2005).
15. G. Gallot and D. Grischkowsky, "Electro-optic detection of terahertz radiation," J. Opt. Soc. Am. B **16**(8), 1204–1212 (1999).
16. J. Lloyd-Hughes, S. P. P. Jones, E. Castro-Camus, K. I. Doig, and J. L. Macmanus-Driscoll, "Modyfying the polarization state of terahertz radiation using anisotropic twin-domains in $LaAlO_3$," Opt. Lett. **39**(5), 1121–1124 (2014).
17. V. Petrov, J.-J. Zondy, O. Bidault, L. Isaenko, V. Vedenyapin, A. Yelisseyev, W. Chen, A. Tyazhev, S. Lobanov, G. Marchev, D. Kolker, "Optical, thermal, electrical, damage, and phase-matching properties of lithium selenoindate," J. Opt. Soc. Am. B **27**(9), 1902–1927 (2010).
18. M. Schall, M. Walther, and P. U. Jepsen, "Fundamental and second-order phonon processes in CdTe and ZnTe," Phys. Rev. B **64**(9), 094301 (2001).
19. W. G. Fateley and F. R. Dollish, *Infrared and Raman Selection Rules for Molecular and Lattice Vibrations: The Correlation Method* (John-Wiley & Sons. Inc., 1972).
20. B. Lorenz, "High pressure Raman investigation of $LiInSe_2$ in the β-$NaFeO_2$ structure," J. Phys. Chem. Solids **58**(3), 399–402 (1996).
21. A. Eifler, V. Riede, S. Wenger, S. Weise, E. Nowak, D. Sprinz, G. Lippold, W. Grill, "Infrared and Raman study of lattice vibrations of $LiInSe_2$ single crystals," Cryst. Res. Technol. **31**, Suppl. 31, 353–356 (1996).
22. M. J. P. Musgrave and J. A. Pople, "A general valence force field for diamond," Proc. R. Soc. Lond. A **268**, 474–484 (1962).
23. H. Neumann, "Lattice vibrations in $A^IB^{III}C_2^{III}$ chalcopyrite compounds," Helv. Phys. Acta **58**, 337–346 (1985).
24. R. M. Martin, "Elastic Properties of ZnS structure semiconductors," Phys. Rev. B **1**(10), 4005–4011 (1970).
25. H. Neumann, "Bond ionicities and structural trends in some $LiB^{III}C_2^{III}$ compounds," Cryst. Res. Technol. **21**(9), 1207–1212 (1986).
26. H. Sobotta, H. Neumann, V. Riede, and G. Kuehn, "Lattice vibrations and interatomic forces in $LiInSe_2$," Cryst. Res. Technol. **21**(10), 1367–1371 (1986).
27. H. Neumann, "Interatomic force constants and localized effective charges in sphalerite-structure compounds," Cryst. Res. Technol. **20**(6), 773–780 (1985).

1. Introduction

THz time-domain spectroscopy (THz-TDS) [1–3] enables the investigation of optical properties of materials in the far-infrared frequency region. It provides a sensitive method for the study of low-frequency transverse optical phonon resonances in crystals. Polarization dependent measurements allow the mapping of the dielectric tensor and to determine the polarization of IR active phonons.

LISe is a nonlinear chalcogenide biaxial orthorhombic crystal with high optical quality [4]. It belongs to $LiB^{III}C_2^{IV}$ family compounds, which exhibit a tetrahedral lattice structure [5]. The structural and electronic properties of LISe have been reported previously [6,7]. Although optical properties of LISe in the mid-infrared range have been studied theoretically and experimentally [8,9], its optical properties in the THz frequency region is not yet completely revealed.

In this paper, we investigate *a*-, *b*- and *c*-cut (*a*, *b* and *c* denote the crystallographic axes of LISe crystal) β-$NaFeO_2$-type LISe single crystals [6,10] and calculate the optical constants such as the refractive index and the absorption coefficient in the frequency range of 0.3 to 2.3 THz using THz-TDS measurements. The orientation dependence of the refractive index of LISe crystal demonstrates significant birefringence in *a*- and *c*-cut crystals and circular-like refractive index ellipsoid in the *b*-cut crystal. Large birefringence of LISe enables phase matching [11], which is essential for THz emission from this crystal. The pronounced absorption of each crystal below 3 THz reflects Se-related lattice vibrations, which agree well with the calculated TO modes in accordance with the valence force field method [12]. Combining the damped multiharmonic oscillator model with the infrared and Raman spectra of LISe crystals cut in different principle axes, the frequency dependent dielectric constants can be obtained with the parameters such as the resonance frequency, damping constant, and oscillator strength.

#208591 - $15.00 USD Received 20 Mar 2014; revised 5 May 2014; accepted 6 May 2014; published 6 Jun 2014

2. Experimental setup and method

Our experiment setup (Fig. 1(a)) employs high-speed asynchronous optical sampling (ASOPS) with two Ti: sapphire femtosecond lasers with repetition rates of approximately 1 GHz [13]. The repetition rate offset of the two lasers is stabilized to 2 kHz by a phase-locked loop. Compared with a mechanical delay line, high-speed ASOPS provides a higher scanning speed and thus a higher sensitivity for ultrafast time-domain spectroscopy. One laser with higher repetition rate serves as pump laser and excites under normal incidence a microstructured large-area photoconductive THz emitter [14]. The emitted THz with linear polarization is collected by the first 90° off-axis parabolic mirror and is then focused onto the sample by the second parabolic mirror. After interacting with the sample, the transmitted THz beam is collimated and focused by the other two parabolic mirrors to a (110) ZnTe detector crystal [15]. The other laser with lower repetition rate serves as probe laser and is overlaid with the THz spot on the detector crystal through a hole in the fourth parabolic mirror. The center wavelength and duration of the pump and probe lasers are approximately 800 nm and 50 fs, respectively. In order to eliminate water absorption in ambient air, the enclosure including the THz beam path is purged with nitrogen gas during the measurement. The probe beam experiences a polarization change due to the THz electric field based on the electro-optic effect in ZnTe. It is focused onto a single detector after passing through a $\lambda/4$ wave plate and a polarization beam splitter. The time-domain signal of sample and reference data are obtained by measuring with and without the sample in the THz beam path, respectively.

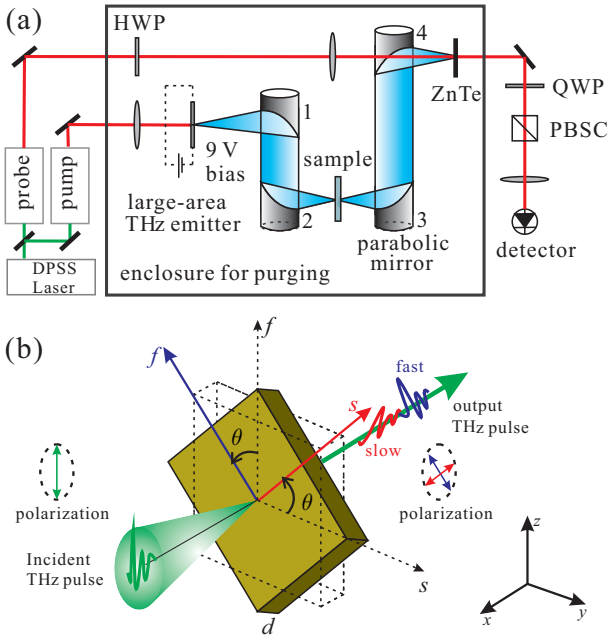

Fig. 1. (a) Schematic sketch of the high-speed ASOPS THz-TDS setup; (b) linear polarized THz beam is split into the fast and the slow components due to birefringence of the crystal.

By performing a Fourier transform to the easily separated main pulse in the transmitted time-domain spectra, the frequency dependence of the refractive index and absorption coefficient of the sample can be quantitatively determined by extracting the amplitude ratio and phase shift

#208591 - $15.00 USD Received 20 Mar 2014; revised 5 May 2014; accepted 6 May 2014; published 6 Jun 2014

between the sample and reference signal:

$$n_S(\omega) = 1 + \frac{\Phi c}{\omega d} \tag{1}$$

$$\alpha_S(\omega) = -\frac{2}{d}\ln\{\frac{[n_S(\omega)+1]^2}{4n_S(\omega)}|T|\} \tag{2}$$

where $|T|$ and Φ are the amplitude and the phase shift extracted from the complex amplitude ratio between frequency-domain spectra of the signal and reference, and c and d are the light speed in vacuum and the thickness of the sample, respectively.

3. Experimental results and discussion

THz transmission spectroscopy of *a*-, *b*- and *c*-cut LISe crystals are measured at room temperature. The LISe crystal is mounted on a 360° rotation stage with its rotation axis parallel to the propagation direction of the THz beam. The THz beam is focused onto the crystal under normal incidence (Fig. 1(b)). Therefore the orientation of the crystal with respect to the incident THz polarization can be manipulated by rotating the crystal. The three crystallographic axes of LISe crystal compose an orthogonal coordinate system. Therefore, if the refractive index is orientation dependent, when a THz pulse is normally incident to a crystallographic plane at an arbitrary angle with respect to one of the two crystallographic axes inside the plane, the incident THz pulse will be separated into two sub-pulses with polarizations perpendicular to each other after passing through the crystal due to the birefringence.

As illustrated in Fig. 1(b), *xyz* is the chosen coordinate system. The *z*-axis polarized THz beam is incident parallel to the *x*-axis and perpendicular to one principle plane of the LISe crystal in the *yz* plane. The transmitted pulse is separated into the fast and the slow pulses. The direction of the polarization of the fast and the slow components are denoted as the f- and the *s*-axis of the crystal, respectively. θ is the angle between the f-axis and the polarization of the incident THz pulse. After propagating through the crystal, the phase delay between the fast and the slow components can be expressed as:

$$\Gamma = \omega d(n_s - n_f)/c \tag{3}$$

where n_f and n_s are the refractive index of LISe crystal along the f- and the *s*-axis, respectively.

To measure the birefringence of the LISe crystal, it is necessary to locate the directions of the f- and the *s*-axis in the *yz* plane. This is realized by rotating the crystal and measuring the position of the THz signal in the time domain. When the f- or the *s*-axis is parallel to the polarization of the incident THz wave, there will be only a single THz pulse in the time domain.

Figure 2 shows the transmitted time- and frequency-domain spectra of the three LISe crystals cut in three principle axes, respectively. From the time-domain spectra of the transmitted THz waves, we can see that the waveform can be modulated by changing the orientation of the crystal with respect to the polarization of the incident THz pulse. The incident single pulse is broken into two pulses with polarizations perpendicular to each other, which is caused by the different group velocities of the fast and the slow components. From the frequency-domain spectra of the transmitted THz waves, we can see a spectral modulation when θ is neither 0° nor 90°. Nonetheless, the spectral modulation will disappear when either the f- or the *s*-axis is parallel to the polarization of the incident THz pulse. Additionally, for *a*- and *c*-cut LISe crystals (Fig. 2(a) and Fig. 2(c)), the amplitude modulation is much more significant than that for *b*-cut LISe crystals.

#208591 - $15.00 USD Received 20 Mar 2014; revised 5 May 2014; accepted 6 May 2014; published 6 Jun 2014

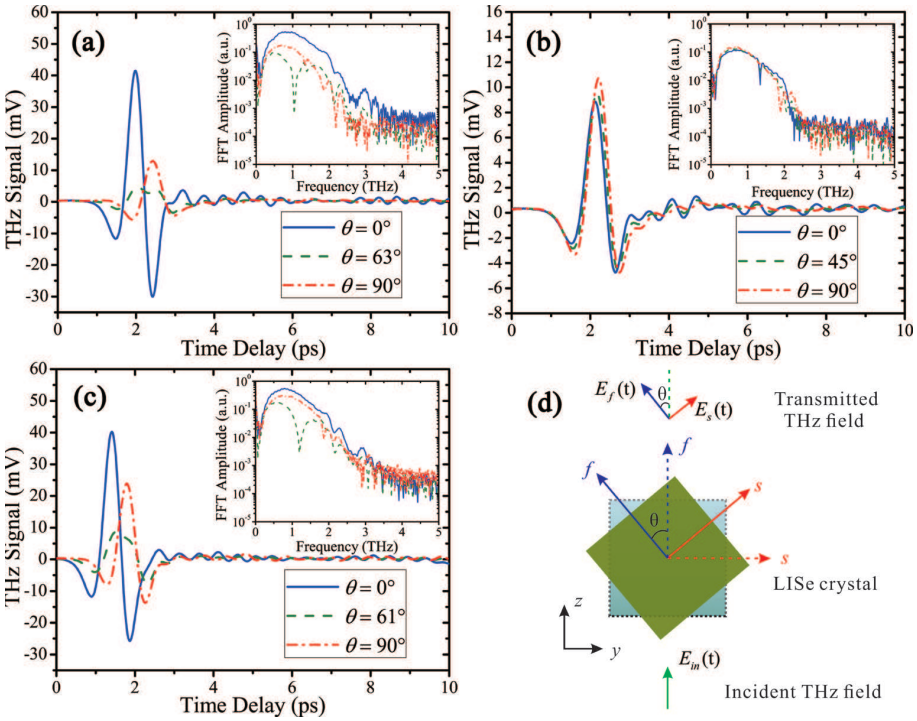

Fig. 2. The transmitted time- and frequency-domain spectra (insets) of (a) *a*-cut LISe crystal with 0.50 mm thickness, (b) *b*-cut LISe crystal with 0.70 mm thickness, (c) *c*-cut LISe crystal with 0.60 mm thickness; (d) orientation illustration of incident THz field, LISe crystal and transmitted THz field.

In LISe crystals, the crystallographic axes *a*, *b* and *c* correspond to its dielectric axes *Y*, *X* and *Z*, respectively. The *X*-, *Y*- and *Z*-axis compose an orthogonal coordinate system, so the refractive indices along the three dielectric axes can be calculated from the transmitted spectra of the crystals. Figure 3(a) illustrates the calculated real part of the refractive index of a LISe crystal when the *X*-, *Y*- and *Z*-axis are parallel to the polarization of the incident THz pulse in accordance with Eq. (1).

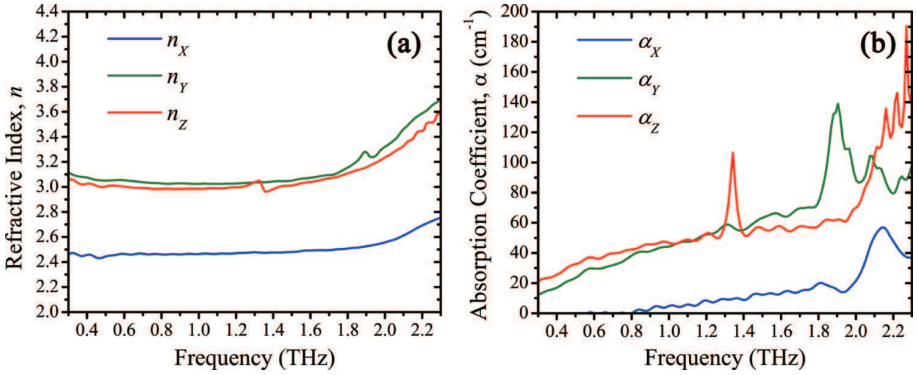

Fig. 3. (a) The refractive index and (b) the absorption coefficient of LISe crystal when the *X*-, *Y*- and *Z*-axis are parallel to the polarization of the incident THz pulse.

#208591 - $15.00 USD Received 20 Mar 2014; revised 5 May 2014; accepted 6 May 2014; published 6 Jun 2014

The refractive indices of the LISe crystal exhibit orientation dependence, which was also observed from the polarization-resolved THz time-domain spectroscopy of $LaAlO_3$ [16]. The values of n_Y and n_Z are very close, which indicates that the refractive index ellipsoid in *b*-cut principle plane is close to circular. Therefore the LISe crystal can be regarded as a quasi-uniaxial crystal in this frequency range. All the three refractive indices n_X, n_Y and n_Z exhibit weak frequency dependence in the whole investigated frequency region except for a dispersive-like feature at around 2.15, 1.90, and 1.34 THz, respectively. In previous work, the refractive indices along the three dielectric axes in the visible region (e.g. at 632.8 nm) were determined as $n_X = 2.387$, $n_Y = 2.435$, $n_Z = 2.437$, respectively [17]. From our measurement, the refractive indices along the three dielectric axes in the far-infrared frequency region (e.g. at 300 μm, i.e. 1 THz) were determined as $n_X = 2.464$, $n_Y = 3.025$, $n_Z = 2.985$, respectively. Obviously, the refractive indices in the far-infrared region are larger than those in visible region. We also calculated the birefringence in *b*-, *a*-, and *c*-cut principle planes at these two wavelengths. The birefringence Δn of LISe in the three principle planes are $|n_Y - n_Z|$, $|n_Z - n_X|$ and $|n_X - n_Y|$, respectively (Table 1).

Table 1. Birefringence of *b*-, *a*-, and *c*-cut principle planes of LISe crystal.

Wavelength	Birefringence Δn		
	b-cut	*a*-cut	*c*-cut
632.8 nm	0.002	0.050	0.048
300.0 μm	0.040	0.521	0.561

As illustrated in Table 1, the birefringence in the THz frequency region is larger than in the visible region in all three orthogonal principle planes of the LISe crystal. As expected the *b*-cut principle plane shows much smaller birefringence than the $a-$ and the $c-$cut principle planes.

Figure 3(b) illustrates the absorption coefficient when the *X*-, *Y*- and *Z*-axis are parallel to the polarization of the incident THz waves on the basis of Eq. (2). Pronounced absorption peaks occur at around 2.15, 1.90 and 1.34 THz in α_X, α_Y and α_Z, respectively. These absorption peaks are attributed to lattice vibrations and are responsible for the dispersive like features in n_X, n_Y and n_Z at the same frequencies. We can also see that α_X shows much smaller values than α_Y and α_Z. Moreover, a slow increase in the absorption coefficient is observed, which stems from the low-frequency wing of higher-frequency TO phonons [18].

LISe with β-$NaFeO_2$ structure containing perfect $InSe_4$ tetrahedrons and weak Li-Se covalent bonds has point group C_{2v}. The Li-related lattice vibrations are corresponding to higher frequencies due to the small mass of Li, so the vibrations in low- and middle-frequency range are only corresponding to In-Se covalent bonds [6].

According to infrared and Raman selection rules [19], the irreducible representation of the optical modes of β-$NaFeO_2$-type LISe can be expressed as:

$$11A_1 \oplus 12A_2 \oplus 11B_1 \oplus 11B_2 \tag{4}$$

where the B_2, B_1 and A_1 optical modes are infrared active for the cases that the *X*-, *Y*- and *Z*-axis are parallel to the polarization of the incident THz pulse, respectively.

Based on the damped multiharmonic oscillator model, the frequency dependence of the complex dielectric constant of LISe crystals is given by [12]:

$$\varepsilon(\nu) = \varepsilon_\infty + \sum_{i=1}^{N} \frac{s_i \nu_{TOi}^2}{\nu_{TOi}^2 - \nu^2 + i\gamma_i \nu} \tag{5}$$

#208591 - $15.00 USD Received 20 Mar 2014; revised 5 May 2014; accepted 6 May 2014; published 6 Jun 2014

and

$$\sum_{i=1}^{N} s_i = \varepsilon_0 - \varepsilon_\infty \tag{6}$$

where ε_∞ and ε_0 are the high- and low-frequency dielectric constant, N the number of transverse optical modes, and s_i, ν_{TOi} and γ_i denote the oscillator strength, the frequency and damping constant of the ith TO mode. With the infrared and Raman spectra of LISe [6,20,21], we can determine the optical lattice modes and calculate the complex dielectric constant, and then obtain the refractive index and the absorption coefficient on the basis of the relations:

$$n = \sqrt{\frac{\sqrt{\varepsilon_r^2 + \varepsilon_i^2} + \varepsilon_r}{2}} \tag{7}$$

$$\alpha = \frac{4\pi\nu}{c}\sqrt{\frac{\sqrt{\varepsilon_r^2 + \varepsilon_i^2} - \varepsilon_r}{2}} \tag{8}$$

where ε_r and ε_i are the real and imaginary parts of the dielectric constant.

Figure 4 illustrates the refractive index and the absorption coefficient calculated from Eq. (5), Eq. (6), Eq. (7) and Eq. (8) by choosing the lowest 5 TO modes for the three cases mentioned above, respectively. The peaks at around 2.13 THz, 2.09 THz and 1.31 THz in α_X, α_Y and α_Z are corresponding to the phonon frequencies observed from X-, Y- and Z-polarized infrared and Raman spectra, respectively. The peak at around 1.90 THz in α_Y is clearly observed in our THz transmission spectra. The parameters used for simulation of the refractive index and the absorption coefficient in Fig. 4 are shown in Table 2 where the oscillator strength s is given in % relative to the phonon mode with the strongest oscillator strength. The damping constant γ is a fit parameter. The theoretical simulation reproduces the calculation from the experimental data well except for a low frequency absorption of about 40 cm^{-1} in α_Y and α_Z. The experimental data show an additional off-set with slight linear increase in absorption. The origin of this difference in absorption may stem from a stronger broadening of high frequency phonon modes (modes above 6 THz are not considered in our model) or impurities, and is under further investigation.

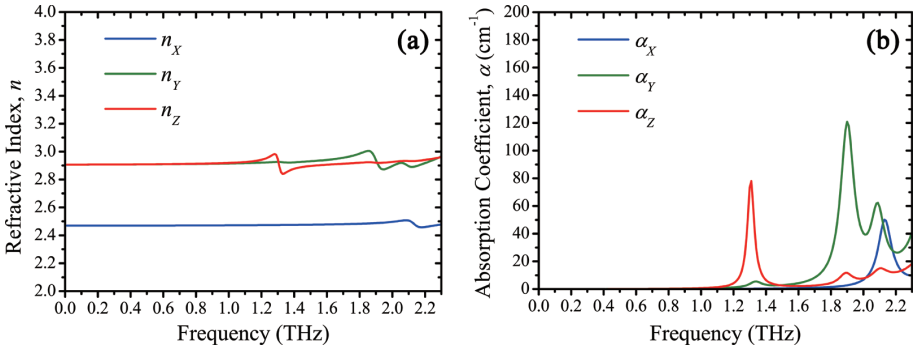

Fig. 4. Simulated refractive index (a) and absorption coefficient (b) of LISe when the X-, Y- and Z-axis are parallel to the polarization of the incident THz pulse.

The frequency of the lattice vibrations are determined by the interatomic forces in the crystal. Without considering the contribution of long-range Coulomb forces to the elastic constants

#208591 - $15.00 USD Received 20 Mar 2014; revised 5 May 2014; accepted 6 May 2014; published 6 Jun 2014

and the influence of the dipole-dipole interactions on the transverse optical mode, the interatomic forces can be decomposed into bond-stretching and bond-bending forces according to the valence-force-field (VFF) approach [12,22]. The force constants in the tetrahedral unity of LISe was described by the Keating model [23], and the relation between TO mode and the force constant is given by [24]:

$$\nu_{TO}^2 = \frac{k_1 + k_2}{m_{\text{eff}}\pi^2} \tag{9}$$

where m_{eff} is the effective mass of the vibration part. k_1 and k_2 are the bond-stretching and bond-bending force constants with the relation $k_2 = 0.28(1-f_i)k_1$, where f_i is the spectroscopic bond ionicity. The necessary parameters for calculating the TO mode using interatomic forces are $k_1 = 43.1$ N/m, $f_i = 0.599$ [25,26].

Suppose that only the Se atoms vibrate with In atoms remaining still, the corresponding TO phonon frequency induced by bond-stretching and bond-bending forces are around 5.77 THz and 1.93 THz, respectively. Therefore the high-frequency vibrational modes are related to bond-stretching forces and the vibrational modes in the three dielectric axes shown in Fig. 3(b) are related to the bond-bending forces of In-Se covalent bonds [27]. The difference of the vibrational frequencies for LISe crystal with X-, Y- and Z-axis parallel to the THz electric field is attributed to the lattice symmetry of β-$NaFeO_2$ structure. Furthermore, the frequency offset between the calculated vibrations and the experimental result is probably due to the exact values of the effective mass and electric forces.

Table 2. Parameters used for simulating the refractive index and the absorption coefficient of LISe with the X-, Y- and Z-axis parallel to the polarization of the incident THz pulse.

axis	ε_0	ε_∞	ν_{TO}(THz)	γ(THz)	s (%)
			2.13	0.10	20
			2.51	0.10	25
X	6.10	5.47	2.69	0.12	15
			3.50	0.13	20
			5.84	0.15	100
			1.34	0.09	2
			1.90	0.10	30
Y	8.45	5.47	2.09	0.10	10
			2.46	0.12	60
			5.24	0.15	100
			1.31	0.05	20
			1.89	0.10	2
Z	8.45	5.25	2.10	0.12	2
			2.58	0.14	60
			4.85	0.15	100

4. Conclusion

In conclusion, we demonstrate significant birefringence of biaxial LISe crystals in the THz frequency range. Both the refractive index and the absorption coefficient of LISe are orientation dependent and the frequencies of the pronounced absorption peaks agree well with the vibrational modes obtained from infrared and Raman spectra. Our investigations of the linear optical properties of LISe in combination with reported nonlinear coefficients suggest that phase matching for THz generation by optical rectification seems feasible. Additionally, the

#208591 - $15.00 USD Received 20 Mar 2014; revised 5 May 2014; accepted 6 May 2014; published 6 Jun 2014

low-frequency vibrational modes below 3 THz mainly stem from bond-bending forces of the In-Se covalent bonds in the LISe crystal.

Acknowledgments

This research is supported by the Center for Applied Photonics (CAP) at the University of Konstanz, the DFG through the SFB 767 (Germany), the China Scholarship Council (CSC), the State National Natural Science Foundation of China (Grant No. 51272129, 5021002) and the 973 Program of the People's Republic of China (Grant No. 2010CB630702).

#208591 - $15.00 USD Received 20 Mar 2014; revised 5 May 2014; accepted 6 May 2014; published 6 Jun 2014